

THERMODYNAMIC ANALYSIS OF A SOLAR-DRIVEN ABSORPTION HEAT TRANSFORMER FOR INDUSTRIAL PROCESS HEAT

Evangelos Bellos¹, Christos Sammouris¹, Panagiotis Lykas¹, Angeliki Kitsopoulou¹, Ioannis Alexopoulos¹, Ahmad Arabkoohsar², Christos Tzivanidis^{1*}

¹National Technical University of Athens, Department of Thermal Engineering, Athens, Greece

²Technical University of Denmark, Department of Civil and Mechanical Engineering, Kgs. Lyngby, Denmark

*Corresponding Author: ctzivan@central.ntua.gr

ABSTRACT

The objective of the present study is to examine a solar-driven absorption heat transformer operating with the LiBr/Water working pair. Selective flat plate solar thermal collectors coupled with an insulated sensible storage tank feed the absorption heat transformer for industrial heat production. Practically, the heat transformer upgrades the solar useful output through a thermochemical absorption cycle. This work uses a validated thermodynamic model developed in Engineering Equation Solver, while the transient investigation is conducted with TRNSYS software by connecting the tools properly, exploiting their interoperability. During this analysis, the impact of different parameters on the system performance is investigated aiming to calculate the industrial heat production and the overall system efficiency. Specifically, the effect of the solar field mass flow rate, the load mass flow rate, the solar field area, and the storage tank volume are calculated. A simulation for a summer week in Athens (Greece) indicates that the use of a 100 m² solar field with a tank of 8 m³ leads to the production of 580 kWh of industrial heat at 120°C. The average coefficient of performance for the heat transformer was found at 0.47, the average solar collector efficiency at 25.6%, the solar to heat conversion efficiency at 12%, and the overall exergy efficiency at 3.1%.

1 INTRODUCTION

Industrial sector decarbonization is a critical issue that has to be properly faced aiming for the sustainability of future societies (Chung *et al.*, 2023). One of the most promising ways to reduce the CO₂ emission of industries and reduce fuel consumption (e.g., natural gas) is the proper exploitation of the waste heat streams (Kosmadakis *et al.*, 2023), as well as the exploitation of renewable energy sources (e.g. solar) (Ghorbani *et al.*, 2021). Waste/renewable heat upgrading (Bai *et al.*, 2023) can be an answer to the challenges that are associated with the industrial energy issue. Heat upgrade aims to increase the temperature of waste or renewable streams to make them suitable for utilization in different industrial processes. There are different upgrading techniques such as heat pumps which need electricity (e.g., from PV) (Tang and Zhang, 2023), and thermochemical upgrading techniques which utilize thermal energy as the driving force (Sarath Babu and Anil Kumar, 2022).

One promising thermochemical heat upgrade technique is absorption heat transformer (AHT) which could have different working pairs but is very commonly based on LiBr/water pair. The LiBr/water AHT exploits medium-temperature heat input (e.g., in the range of 60 to 100°C) and produces useful industrial heat in greater temperatures (e.g., 120 to 165°C (Cudok *et al.*, 2021)). Usually, the efficiency of the machine is close to 0.5 with a mean usual value of 0.47 (Cudok *et al.*, 2021). AHTs face some limitations which are associated with corrosion and crystallization problems.

There are plenty of literature studies about waste heat-driven AHTs. Horuz and Kurt (2010) studied an AHT in a textile industry driven by the warm water of 90°C for upgrading to 120°C for reuse in a dyeing process achieving a coefficient of performance (COP) of about 0.48. However, there is a lack of studies on the investigation of solar heat upgrading by an AHT. Liu *et al.* (2017) studied the heat upgrade of a solar-boiler unit with evacuated tube collectors coupled to an AHT and they found the exergy performance of the unit at 32%. Moreover, a double-stage AHT driven by evacuated tube collectors was studied by Wang *et al.* (2019) finding an energetic performance of close to 20% for that. Furthermore, the investigation of a system with AHT, flat plate collectors, and a compression refrigeration unit was analyzed by Chaiyat and Kiatsiriroat (2014). They concluded that the COP can be increased from 0.49 at the system without compression up to 0.71 with compression.

The objective of the present work is to examine in detail the behavior of a solar-driven AHT with LiBr/water working pair for a week period for industrial heat production. The basic idea is to use flat plate collectors for heating production and coupling them with an AHT for upgrading the heat and making it suitable for industrial use. The novelty of the present study lies in the utilization of an AHT, instead of the widely-used vapor compression heat pumps, and its analysis under both steady-state and transient conditions. This work includes a basic thermodynamic analysis of the AHT for different operating conditions with a validated model by using literature data. Specifically, the thermodynamic analysis is conducted with a homemade model in the Engineering Equation Solver (EES), while the hourly-based investigation is done by TRNSYS. These tools are properly connected to rigorously simulate the integrated system. The transient analysis is performed for a week period in the summer in Athens, Greece. There is also a detailed parametric investigation of the configuration by examining the impact of various design parameters on high-temperature heat production.

2 MATERIALS AND METHODS

2.1 The studied configuration

In the present work, a solar-driven AHT is studied for industrial heating production. The studied unit is depicted in **Figure 1** where all the details about the connection of the different devices are reported. The flat plate solar thermal collectors produce useful heat which is stored in an insulated storage tank, and it feeds the evaporator and the generator of the AHT with heat input in a medium temperature (T_m). The AHT exploits this heat input and upgrades a part of the heat input to high-temperature heat of temperature (T_{heat}) for industrial utilization. The AHT operates with LiBr/water working pair, which is always kept in the liquid phase avoiding crystallization which could damage the device. Moreover, the heat transfer fluid in the solar field/tank part is pressurized water of 10 bar to be kept at the liquid phase up to 180°C. Practically, lower temperature levels are expected during the operation. It is valuable to state that the AHT needs heat input in the evaporator and the generator, while the condenser rejects heat to the ambient and the absorber produces useful heat for industrial utilization.

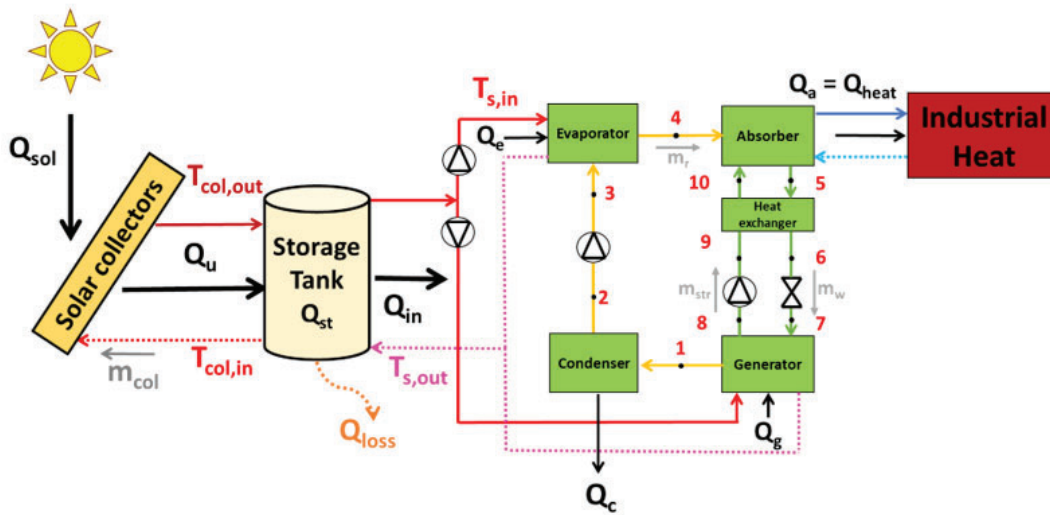


Figure 1: The investigated solar-driven AHT for industrial heating production

2.2 Basic Mathematical Background

The thermal efficiency of the selective flat plate collector is calculated using the Equation (1) (Bellos *et al.*, 2022):

$$\eta_{th,col} = \frac{Q_u}{Q_{sol}} = 0.77 - 3.75 \cdot \frac{T_{col,in} - T_{am}}{G_T} - 0.015 \cdot \frac{(T_{col,in} - T_{am})^2}{G_T} \quad (1)$$

The incident angle modifier at 50° is set at 88% as a typical value. The solar energy input is calculated using the Equation (2):

$$Q_{sol} = A_{col} \cdot G_T \quad (2)$$

The useful heat production by the solar field is calculated using the Equation (3):

$$Q_u = m_{col} \cdot c_p \cdot (T_{col,out} - T_{col,in}) \quad (3)$$

The useful heat production can also be calculated based on the energy balance of the source volume, using the Equation (4):

$$Q_{in} = m_s \cdot c_p \cdot (T_{s,in} - T_{s,out}) \quad (4)$$

The generalized energy balance in the storage tank can be calculated using the Equation (5):

$$Q_{st} = Q_u - Q_{in} - Q_{loss} \quad (5)$$

The thermal losses of the tank are calculated by considering a thermal loss coefficient of $U_t=0.2 \text{ W/m}^2\text{K}$, assuming a well-insulated tank. In this analysis, TRNSYS uses the mixing zone modeling, and a total of 7 thermal zones were selected.

In the AHT, the heat input is given in the same temperature level, thus $T_m=T_c=T_g$, while the heating is produced in $T_{heat}=T_a$. The gross temperature lift (GTL) is calculated as $GTL=T_{heat}-T_{am}$. The total heat input in the AHT is the sum of the heat input in the evaporator and in the condenser, specifically: $Q_{in}=Q_c+Q_g$.

The energy balances in the basic devices of the AHT are listed in Equations (6) to (10) shown below:

$$\text{Evaporator:} \quad Q_e = m_r \cdot (h_4 - h_3) \quad (6)$$

$$\text{Generator:} \quad Q_g = m_r \cdot h_1 + m_s \cdot h_8 - m_w \cdot h_7 \quad (7)$$

$$\text{Condenser:} \quad Q_c = m_r \cdot (h_1 - h_2) \quad (8)$$

$$\text{Absorber:} \quad Q_a = m_r \cdot h_4 + m_s \cdot h_{10} - m_w \cdot h_5 \quad (9)$$

$$\text{Heat exchanger:} \quad m_s \cdot (h_{10} - h_9) = m_w \cdot (h_5 - h_6) \quad (10)$$

The mass flow rate in the generator regarding the total mass and the LiBr mass are given below in Equations (11) and (12) respectively:

$$m_w = m_{str} + m_r \quad (11)$$

$$m_w \cdot X_w = m_{str} \cdot X_{str} \quad (12)$$

The expansion in the throttling valve is conducted without losses, thus $h_7=h_6$. Also, the work input in the circulation pumps is extremely small, thus $h_9=h_8$ and $h_3=h_2$. Also, the heat exchanger's effectiveness is chosen at 70% (Rivera *et al.*, 2003).

The pinch point in the generator and the evaporator was selected at 3 K, while the condenser temperature was selected at 7 K greater than the ambient temperature. The energy balance of the source steam can be written using the Equation (13) shown below:

$$Q_{in} = m_s \cdot c_p \cdot (T_{s,in} - T_{s,out}) \quad (13)$$

The AHT's COP is calculated using the Equation (14):

$$COP = \frac{Q_{heat}}{Q_{in}} \quad (14)$$

The exergy efficiency of the AHT, taking into account its exergy input, and output rate, is calculated using Equation (15) below:

$$\eta_{ex,AHT} = COP \cdot \frac{1 - \frac{T_{am}}{T_{heat}}}{1 - \frac{T_{am}}{T_m}} \quad (15)$$

The system energy efficiency is defined as the ratio of the produced heating to the solar energy input as shown in Equation (16) below:

$$\eta_{en,sys} = \frac{Q_{heat}}{Q_{sol}} \quad (16)$$

The system exergy efficiency is defined as, using the Petela model (Petela, 2003) as shown in Equation (17), temperatures in Kelvin and $T_{sun}=5770$ K.

$$\eta_{ex,sys} = \frac{Q_{heat} \left(1 - \frac{T_{am}}{T_{heat}}\right)}{Q_{sol} \left[1 - \frac{4}{3} \left(\frac{T_{am}}{T_{sun}}\right) + \frac{1}{3} \left(\frac{T_{am}}{T_{sun}}\right)^4\right]} \quad (17)$$

2.3 Simulation Strategy

In this work, the thermodynamic model was developed with EES (“EES: Engineering Equation Solver”), while the transient analysis was done with the TRNSYS (TRNSYS | Transient System Simulation Tool”), by properly connecting these tools. In the thermodynamic analysis, different combinations of the (T_m) and the (GTL) were studied with the ($T_c=35^\circ\text{C}$), while the COP and the exergy efficiency of the AHT were calculated. Regarding the TRNSYS model, the solar thermal collectors were modeled with Type 1, the storage tank with Type 4, the pumps with Type 3, the EES cycle with Type 66, and the controls were designed with a combination of various types like Type 672 (thermostat), Type 2 (Differential Controller), while the proper printers were used (Type 65). The time step was selected at 5 min, after a proper sensitivity analysis, and the initial temperature values were chosen after some initial iterations for convergence.

The analysis was performed for a summer week in Athens (Greece) specifically from the 13 up to 19 of July (7 days – 168 hours). In the transient analysis, a case study about the AHT was selected, while the emphasis was given to the proper selection of different design parameters of the overall solar-driven unit. **Table 1** summarizes the values of the examined parameters in the benchmark scenario of this work.

Table 1: Basic input values of the present work in the benchmark scenario

Parameters	Values
Collecting area	100 m ²
Collector slope	30°
Collector azimuth angle	0°
Storage tank volume	8 m ³
Tank thermal loss coefficient	0.2 W/m ² K
Solar field mass flow rate	1 kg/s
Load mass flow rate	0.15 kg/s
Pinck point in the generator/evaporator	3 K
Condenser temperature over the ambient	7 K
Heat exchanger effectiveness in the AHT	70%
Default AHT generator/evaporator temperature	80°C
Default heating production temperature	120°C

2.4 Validation of absorption heat transformer model

The created thermodynamic model of the AHT was validated by using literature data from the research work of Rivera *et al.* (2003). **Table 2** gives the comparison data between the literature and the model. The mean deviation of the COP was calculated at 1.5%, which is a small and acceptable value.

Table 2: Comparison data about the COP between this work and the research work of Rivera *et al.* (2003)

T_c (°C)	T_a (°C)	$T_c=T_g$ (°C)	COP (Literature)	COP (This study)	Deviation
20	121	74.1	0.4824	0.4876	1.08%
22	121	74.1	0.4787	0.4824	0.77%
24	121	74.1	0.4713	0.4752	0.83%
26	121	74.1	0.4614	0.4643	0.63%
28	121	74.1	0.4454	0.4453	0.02%
30	121	74.1	0.4082	0.4017	1.59%

20	125	74.1	0.4713	0.4779	1.40%
22	125	74.1	0.4664	0.4682	0.39%
24	125	74.1	0.4503	0.4522	0.42%
26	125	74.1	0.4243	0.4199	1.04%
28	125	74.1	0.3402	0.3135	7.85%
20	129	74.1	0.4540	0.4590	1.10%
22	129	74.1	0.4342	0.4346	0.09%
24	129	74.1	0.3860	0.3734	3.26%

3 RESULTS AND DISCUSSION

3.1 Thermodynamic analysis of the absorption heat transformer

The first step in this work is the presentation of the thermodynamic performance of the AHT. **Figure 2** shows the COP of the AHT, while **Figure 3** depicts the exergy efficiency of this device. The results are presented for different combinations of the heat input temperature (T_m) and the gross lift temperature, while the condenser temperature is set at $T_c=35^\circ\text{C}$. The COP was found to be up to 0.5 which is a reasonable value according to the usual reported values in the literature (Cudok *et al.*, 2021). Indicatively, for the case of $T_m=80^\circ\text{C}$, the COP keeps high values for GTL up to 40 K, while for $T_m=100^\circ\text{C}$ the COP is high GTL up to 60 K. The results regarding the exergy efficiency indicate relatively high exergy efficiency values for the AHT. This index evaluates the AHT in exergetic terms separately, without taking into account the significant exergy losses due to the solar heat provision. Indicatively, for $T_m=80^\circ\text{C}$, the maximum exergetic efficiency is 73.99% for GTL=40 K, for $T_m=90^\circ\text{C}$, the maximum exergetic efficiency is 74.32% for GTL=50 K (global maximum exergy value), while for $T_m=100^\circ\text{C}$, the maximum exergetic efficiency is 74.20% for GTL=60 K.

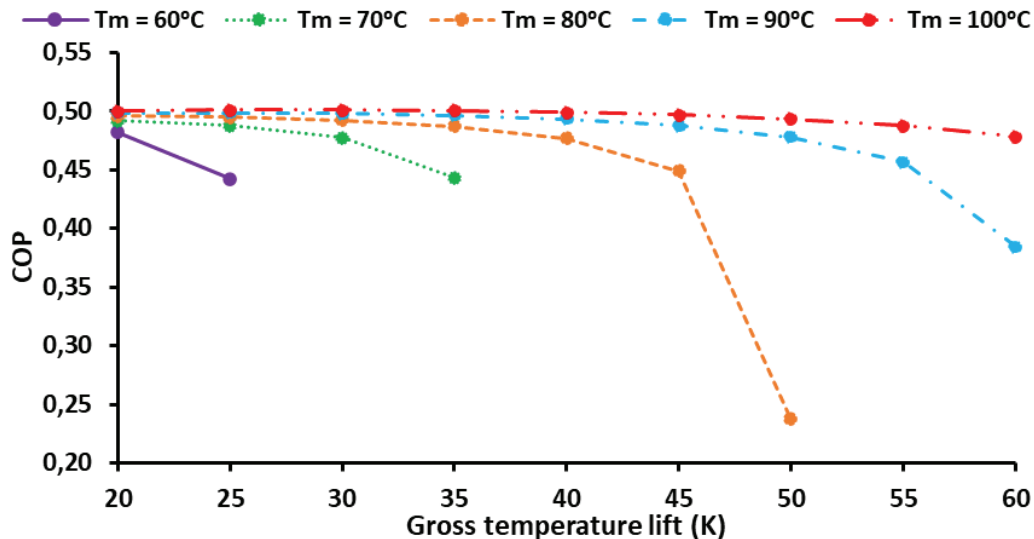


Figure 2: COP of the AHT for various operating scenarios

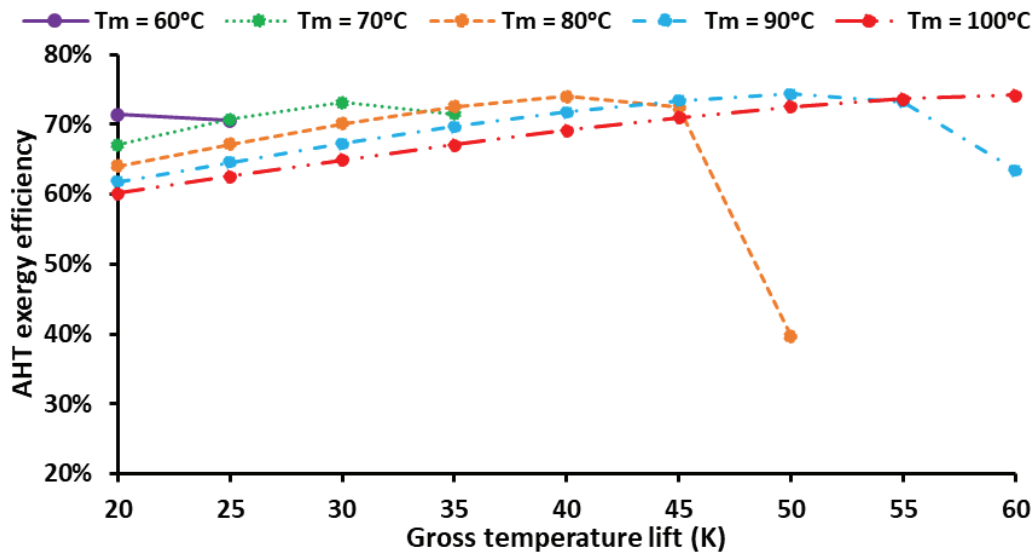


Figure 3: AHT exergy efficiency for various operating scenarios

3.2 Transient investigation of solar-driven system

The transient investigation is conducted for a week in July and for $T_m=80^\circ\text{C} - T_{heat}=120^\circ\text{C}$. Figure 4 illustrates heat rate flows for the heating production, the heat input in the AHT, the useful heat production from the solar field, and the solar irradiation on the collectors. Similar profiles are reported for all the examined days because all these days are sunny days with adequate solar potential to ensure a stable operation. It is notable to state that the solar energy rate is noticeably larger rate than the others. Moreover, it is interesting to state that the input heat rate in the AHT and the associated heating input are maximized later than the solar noon due to the thermal storage tank that manages properly the useful heat production.

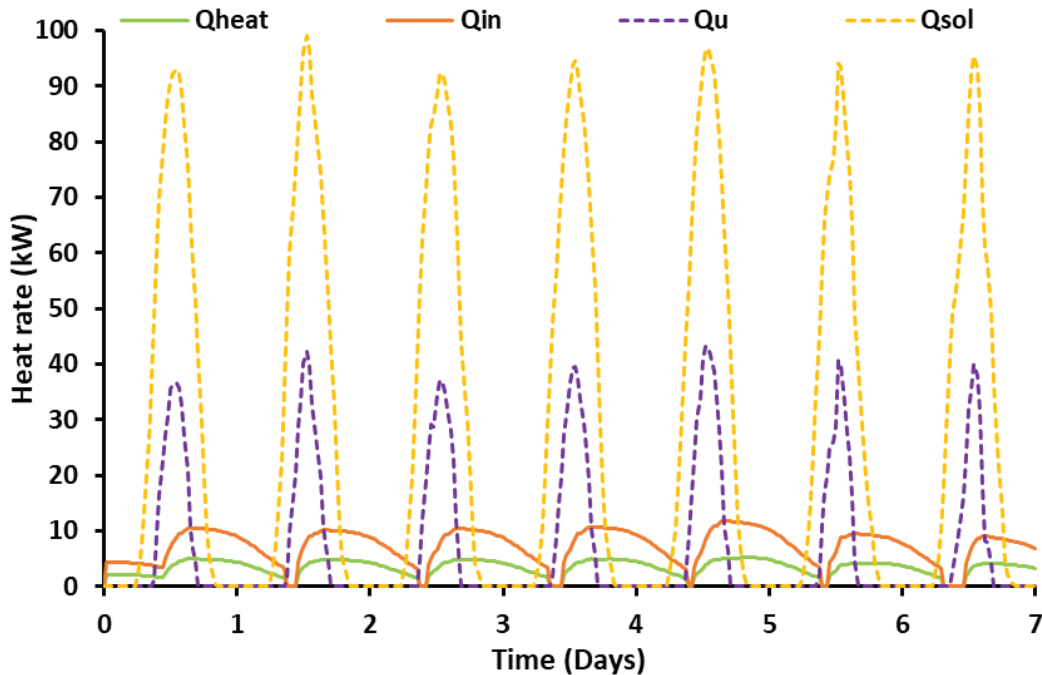


Figure 4: Heat rate variation for the heating production, the heat input in the AHT, the solar field useful heat product, and the solar energy input for the examined summer week

Figure 5 exhibits the temperature rates associated with the solar field and the source stream with AHT. It is obvious that the maximum collector outlet temperature is close to 100°C, while the maximum inlet temperature is close to 95°C, having a temperature lift around 5 K which is a reasonable value. The temperature levels of the source to the AHT ($T_{s,in}$) follow the outlet temperature of the collector up to the moment that the solar field stops operating. After that point, the discharge process is performed and the ($T_{s,in}$) presents a decreasing rate, while the AHT continues to produce heating. The return temperature from the AHT to the tank ($T_{s,out}$) is controlled at 83°C when there is operation when it is equal to the ($T_{s,in}$) when the AHT stops its operation.

Figure 6 depicts the basic performance indexes of the AHT and of the solar field. The solar thermal efficiency has a significant variation during the day, reaching up to 40-45% close to noon. On the other hand, the COP of the AHT has a rough variation which is explained by the variation of the ambient temperature which is associated with the condenser's temperature. Generally, the COP is found to be a bit lower than 0.5, which is an acceptable value for an AHT.

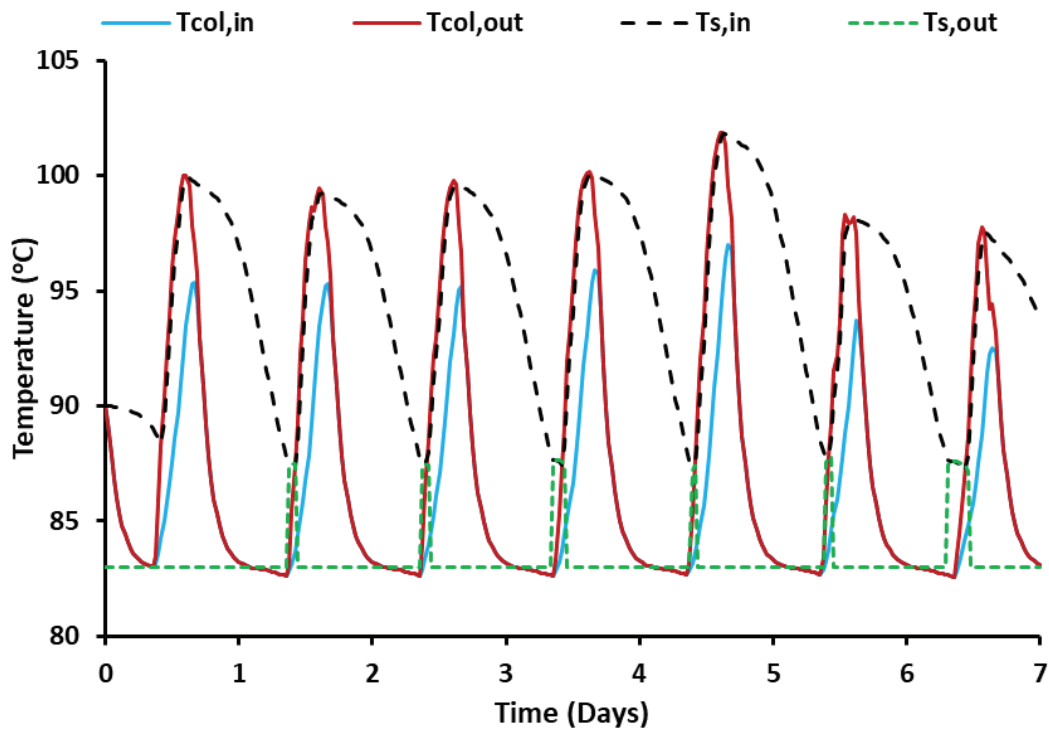


Figure 5: The temperature levels variation in the collector inlet and outlet, and in the source inlet and outlet from the AHT for the examined summer week

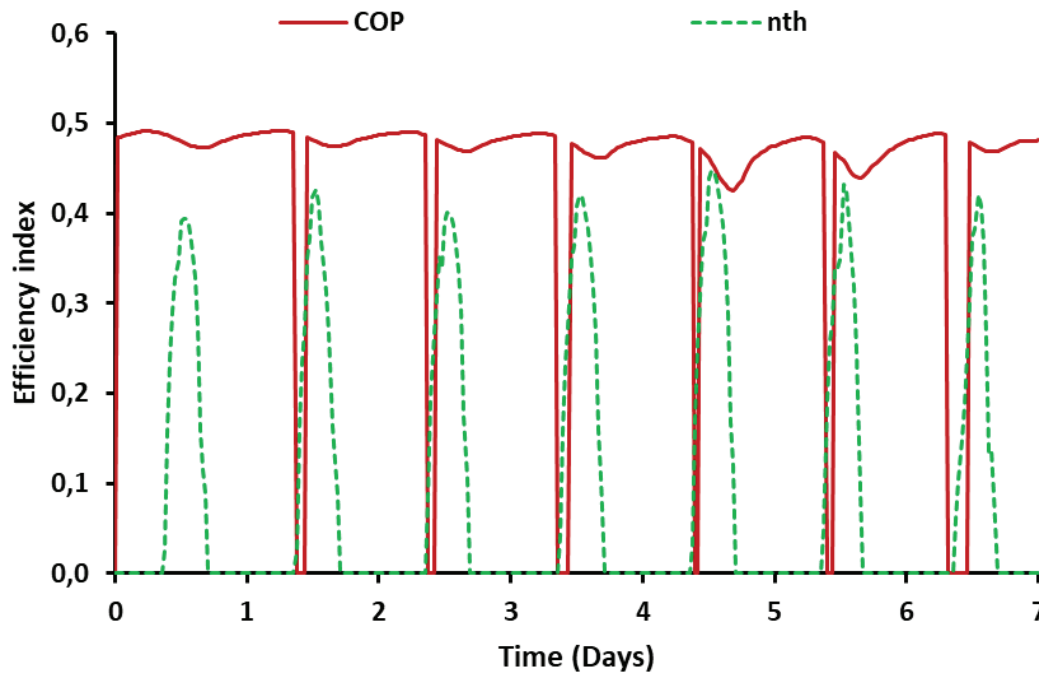


Figure 6: The AHT COP and the collector solar thermal efficiency variation for the examined summer week

Table 3 summarizes the weekly data of the examined unit. The heating production at 120°C is found to be 580 kWh, the mean AHP COP 0.4744, the solar thermal mean efficiency 25.61%, the mean system energy efficiency 11.99%, and the mean system exergy efficiency 3.07%.

Table 3: Summary of the weekly results of the transient analysis with ($T_m=80^\circ\text{C} - T_{\text{heat}}=120^\circ\text{C}$)

Parameters	Values
Industrial heat production	580 kWh
Energy input in the AHT	1223 kWh
Useful heat production by the solar field	1239 kWh
Solar energy input in the system	4837 kWh
Mean AHP COP	0.4744
Mean solar thermal efficiency	25.61%
Mean system energy efficiency	11.99%
Mean system exergy efficiency	3.07%

The last part of this section includes results regarding the parametric analyses of the overall unit for the studied week. The influence of different parameters is depicted in **Figure 7**. It is obvious that the increase of the solar field area increases the heat production, while the increase of the mass flow rate reduces the production. Practically higher collecting area increases the solar heat input in the system, something that makes possible higher productivity. On the other hand, the increase of the solar field mass flow rate creates some control issues that are associated with the local cold of the water at the start/stop of the system. In any case, the impact of the mass flow rate of the solar field has a relatively small impact on the performance.

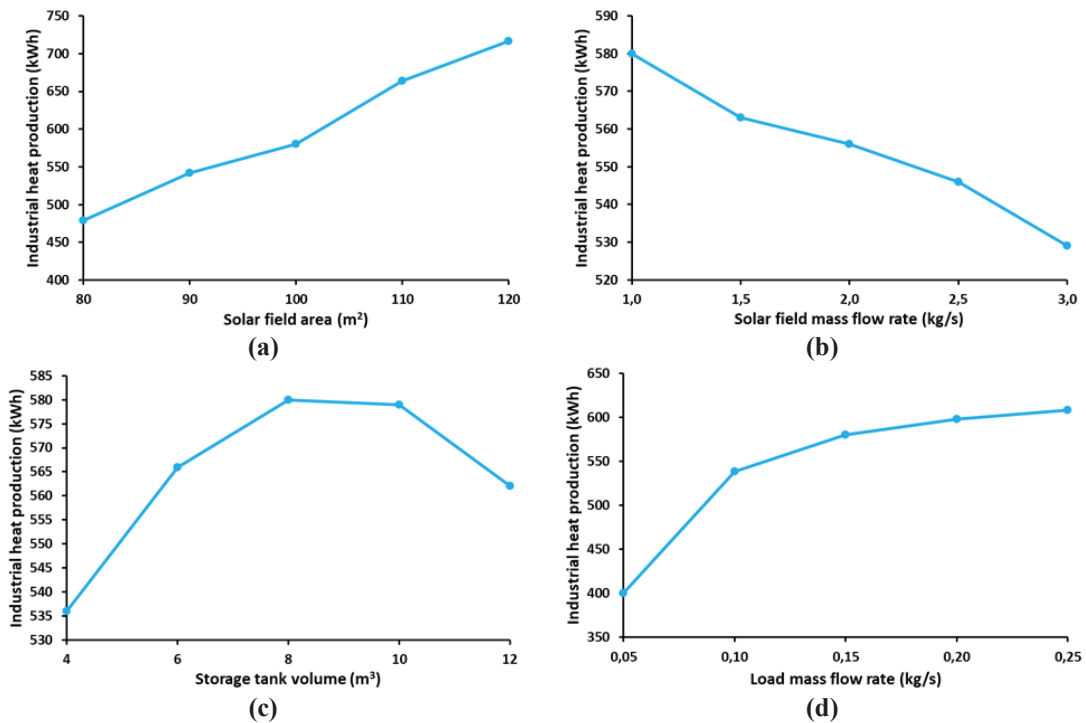


Figure 7: The variation of the industrial heat production by the variation of different parameters named as (a) solar field area, (b) solar field mass flow rate, (c) storage tank volume, and (d) load mass flow rate

The next studied parameter in **Figure 7** is the storage tank volume and it is clear that there is an optimal region that maximizes the heating production. The optimal region is in the range of 8 to 10 m³, while the global maximum value is at 8 m³. Practically, the increase of the storage tank volume gives the possibility for storing higher amounts of thermal energy, but after a limit, the thermal losses increase and make the further increase not beneficial. These factors explain the existence of an intermediate optimal tank volume. The last examined parameter is the source mass flow rate to the AHT and it is concluded that its increase leads to a rise in productivity. However, after a limit (e.g., 0.15 kg/s), the rise of productivity is not high and there is not any meaning to increase the mass flow rate.

4 CONCLUSIONS

The goal of the present paper is the investigation of a solar-driven absorption heat transfer for industrial heating. The system was analyzed thermodynamically with EES, and the hourly-based analysis was conducted by connecting EES and TRNSYS software. The key conclusions are highlighted hereunder:

- Regarding the AHT, the global maximum exergy efficiency is found at 74.3% for $T_m=90^\circ\text{C}$ and $GTL=50\text{ K}$.
- The hourly-based analysis throughout an entire week of operation proved that the heat production at 120°C is achieved at a COP of 47.4%, a solar thermal mean efficiency of 25.6%, a mean energy efficiency of 12%, and a mean exergy efficiency of 3.1%.
- The parametric analysis proved that the optimal thermal tank volume is found to be at 8 m³, while the optimal range is generally from 8 up to 10 m³.
- The parametric analysis proved that the productivity of the system increases with the enlargement of the solar field, reduces with the increase of the solar working fluid flow rate, and goes up with the growth of the source flow rate.

In the future, there is a need to conduct a more detailed multi-parametric investigation by also considering different temperature levels in the AHT. Also, economic and environmental investigations of the proposed system here should be conducted aiming to quantify its sustainability level compared to the competing technologies.

NOMENCLATURE

An	Area	(m ²)
C	Specific heat capacity	(J/kg/K)
G	Solar irradiance	(W/m ²)
h	Specific enthalpy	(J/kg)
m	Mass flow rate	(kg/s)
Q	Heat rate	(W)
T	Temperature	(°C)
U	Thermal loss coefficient	(W/m ² /K)
X	Mass fraction	(kg _{LiBr} /kg _{mixture})

Subscript

a	absorber
am	ambient
c	condenser
col	collector
e	evaporator
en	energy
ex	exergy
g	generator
heat	high-temperature heat
in	inlet
loss	losses
m	medium
out	outlet
p	constant pressure
r	refrigerant
s	source
str	strong
sol	solar
st	store
sun	sun
sys	system
T	perpendicular to the aperture
t	tank
th	thermal
u	useful
w	weak mixture

Greek symbols

η	Efficiency
--------	------------

Abbreviations

AHT	Absorption Heat Transformer
COP	Coefficient of Performance
EES	Engineering Equation Solver
GTL	Gross Temperature Lift

REFERENCES

- Bai, T., Qi, Y., Li, Z., Xu, D., 2023, Digital economy, industrial transformation and upgrading, and spatial transfer of carbon emissions: The paths for low-carbon transformation of Chinese cities, *J. Environ. Manage.*, vol. 344, 118528 p.
- Bellos, E., Papavasileiou, L., Kekatou, M., Karagiorgas, M., 2022, A Comparative Energy and Economic Analysis of Different Solar Thermal Domestic Hot Water Systems for the Greek Climate Zones: A Multi-Objective Evaluation Approach, *Appl. Sci.*, vol. 12, 4566 p.
- Chaiyat, N., Kiatsiriroat, T., 2014, Simulation and experimental study of solar-absorption heat transformer integrating with two-stage high temperature vapor compression heat pump, *Case Stud. Therm. Eng.*, vol. 4, p. 166–174.
- Chung, C., Kim, J., Sovacool, B.K., Griffiths, S., Bazilian, M., Yang, M., 2023, Decarbonizing the chemical industry: A systematic review of sociotechnical systems, technological innovations, and policy options, *Energy Res. Soc. Sci.*, vol. 96, 102955 p.
- Cudok, F., Giannetti, N., Ciganda, J.L.C., Aoyama, J., Babu, P., Coronas, A., Fujii, T., Inoue, N., Saito, K., Yamaguchi, S., Ziegler, F., 2021, Absorption heat transformer - state-of-the-art of industrial applications, *Renew. Sustain. Energy Rev.*, vol. 141, 110757 p.
- EES: Engineering Equation Solver [Computer software], *F-Chart Softw.*, URL: <https://fchartsoftware.com/ees/>
- Ghorbani, B., Mehrpooya, M., Karimian Bahnamiri, F., 2021, An integrated structure of bio-methane/bio-methanol cogeneration composed of biogas upgrading process and alkaline electrolysis unit coupled with parabolic trough solar collectors system, *Sustain. Energy Technol. Assess.*, vol. 46, 101304 p.
- Horuz, I., Kurt, B., 2010, Absorption heat transformers and an industrial application, *Renew. Energy*, vol. 35, no. 10, p. 2175–2181.
- Kosmadakis, G., Meramveliotakis, G., Bakalis, P., Neofytou, P., 2023, Waste heat upgrading with high-temperature heat pumps for assisting steam generation in ships: performance, cost and emissions benefits, *Appl. Therm. Eng.*, vol. 236, 121890 p.
- Liu, F., Sui, J., Liu, T., Jin, H., 2017, Energy and exergy analysis in typical days of a steam generation system with gas boiler hybrid solar-assisted absorption heat transformer, *Appl. Therm. Eng.*, vol. 115, p. 715–725.
- Petela, R., 2003, Exergy of undiluted thermal radiation. *Sol. Energy*, vol. 74, no. 6, p. 469–488.
- Rivera, W., Cerezo, J., Rivero, R., Cervantes, J., Best, R., 2003, Single stage and double absorption heat transformers used to recover energy in a distillation column of butane and pentane, *Int. J. Energy Res.*, vol. 27, no. 14, p. 1279–1292.
- Sarath Babu, K., Anil Kumar, E., 2022, A novel cascade resorption system for high temperature thermochemical energy storage and large temperature lift energy upgradation, *Int. J. Hydrog. Energy*, vol. 48, no. 96, p. 37968-37980.
- Tang, C., Zhang, Q., 2023, Green Electrification of the Chemical Industry Toward Carbon Neutrality, *Engineering*.
- TRNSYS | Transient System Simulation Tool [Computer software], *Thermal Energy System Specialists, LLC*, URL: <https://www.trnsys.com/>
- Wang, H., Li, H., Wang, L., Bu, X., Zeng, J., Xie, N., Xu, Q., 2019, A solar-assisted double absorption heat transformer: Off-design performance and optimum control strategy, *Energy Convers. Manag.*, vol. 196, p. 614–622.

ACKNOWLEDGEMENT

This work has been carried out in the framework of the European Union's Horizon Europe programme under grant agreement No. 101103966 (Thermochemical Heat Recovery and Upgrade for Industrial Processes – TechUPGRADE).